Materials Horizons

ROYAL SOCIETY OF CHEMISTRY

COMMUNICATION

View Article Online
View Journal | View Issue

Check for updates

Cite this: *Mater. Horiz.*, 2023, **10**, 4960

Received 3rd July 2023,
Accepted 26th July 2023

DOI: 10.1039/d3mh01020a

rsc.li/materials-horizons

Supraparticles on beads for supported catalytically active liquid metal solutions – the SCALMS suprabead concept†

Thomas Zimmermann, ‡[a] Nnamdi Madubuko,‡[b] Philipp Groppe,‡[a] Theodor Raczka,[a] Nils Dünninger,[ab] Nicola Taccardi,[b] Simon Carl,[c] Benjamin Apeleo Zubiri,[c] Erdmann Spiecker,[c] Peter Wasserscheid,[bde] Karl Mandel,[af] Marco Haumann *[bg] and Susanne Wintzheimer *[af]

A novel GaPt-based supported catalytically active liquid metal solution (SCALMS) material is developed by exploiting the suprabead concept: Supraparticles, *i.e.* micrometer-sized particles composed of nanoparticles assembled by spray-drying, are bonded to millimeter-sized beads. The suprabeads combine macroscale size with catalytic properties of nanoscale GaPt particles entrapped in their silica framework.

At least one catalytic step is required in the fabrication of more than 85% of all chemical products in our daily lives.[1] Therefore, it is evident that catalysis plays a major role in successfully implementing the sustainable use of resources and preserving of our environment. Catalysis helps reduce energy demands in the production of fuels and chemicals. It supports the conversion of renewable energy resources, is crucial for energy storage, and enables the purification of air as well as water.[2,3] Most catalytic processes are heterogeneous, meaning that the reaction in the gas or liquid phase occurs at the surface of a catalyst possessing a different aggregate state.[1] Consequently, there has been and continues to be a continuously ever-growing demand for new catalyst materials for a sustainable future. For this, creative concepts that go beyond traditional strategies are highly needed.[4,5] Heterogeneous catalysts often consist of a catalytically active material such as metallic nanoparticles supported by a high specific surface area material like porous alumina or silica.[6,7] While the support material has no catalytic properties, it can ensure retrievability of the catalyst material from a reaction medium or prevent coalescence (and deactivation) of catalytically

New concepts

In this work, it is proposed for the first time to lift the size of micrometer-scaled particles by supporting them on a millimeter-sized bead to create advanced catalyst-support entities, called suprabeads. This approach increases the size of the units while maintaining the unique properties of the micron-sized particles. While this idea is familiar for supported nanoparticles, attaching μm-particles to a support material requires completely dissimilar, novel synthetic procedures because of the different size regimes and thus, dissimilar physicochemical forces involved in binding the individual species. This concept extends the applicability of μm-scale particles in catalysis and many other fields. Here, it was implemented to synthesize a catalyst-support unit in which catalytically active μm-sized supraparticles are supported on mm-beads. The supraparticles, which represent a relatively recent and unique class of multifunctional materials, consist of assembled SiO_2 and Ga (or GaPt) nanoparticles. Additionally, the possibility to spray-dry gallium dispersions to create supraparticles with enclosed gallium particles or droplets, depending on the temperature of the environment, was shown for the first time. This offers a new approach for generating catalytically active materials.

[a] *Department of Chemistry and Pharmacy, Inorganic Chemistry, Friedrich-Alexander Universität Erlangen-Nürnberg, Egerlandstrasse 1, 91058 Erlangen, Germany*
[b] *Lehrstuhl für Chemische Reaktionstechnik (CRT), Friedrich-Alexander-Universität Erlangen-Nürnberg, Egerlandstrasse 3, 91058 Erlangen, Germany. E-mail: susanne.wintzheimer@fau.de*
[c] *Institute of Micro- and Nanostructure Research (IMN) & Center for Nanoanalysis and Electron Microscopy (CENEM), Interdisciplinary Center for Nanostructured Films (IZNF), Department of Materials Science and Engineering, Friedrich-Alexander-Universität Erlangen-Nürnberg, Cauerstrasse 3, 91058 Erlangen, Germany. E-mail: marco.haumann@fau.de*
[d] *Erlangen Catalysis Resource Center and Interdisciplinary Center for Interface-Controlled Processes, Friedrich-Alexander-Universität Erlangen-Nürnberg, 91058 Erlangen, Germany*
[e] *Forschungszentrum Jülich, "Helmholtz-Institute Erlangen-Nürnberg for Renewable Energies" (IEK 11), Egerlandstr. 3, 91058 Erlangen, Germany*
[f] *Fraunhofer-Institute for Silicate Research ISC, Neunerplatz 2, D97082 Würzburg, Germany*
[g] *Research Centre for Synthesis and Catalysis, Department of Chemistry, University of Johannesburg, P.O. Box 524Auckland Park 2006, South Africa*

† Electronic supplementary information (ESI) available: Experimental section, spray-drying scheme, dynamic light scattering measurements, transmission electron microscopy, nano-CT projection, laser diffraction measurements, ICP results, SEM studies, nitrogen sorption measurements, reactor flow scheme, propane dehydrogenation experiments, temperature programmed oxidation measurements, ESI Video 1: HRES PC nano-CT tilt series (supraparticles as prepared), ESI Video 2: virtual reconstructed slices of HRES PC nano-CT tilt series, ESI Video 3: 3D visualization of HRES PC nano-CT tilt series. See DOI: **https://doi.org/10.1039/d3mh01020a**

‡ These authors contributed equally to this work.

active nanoparticles. Thus, in the design of high-performance catalysts, both the active material and the support must interact optimally.

In the last 15 years, the concept of considering nanoparticles as building blocks to create more complex particulate units has gained increasing attention.[8] Such entities can be termed supraparticles[9] and may represent a smart method for the creation of heterogeneous catalysts. Compared to nanoparticles and macroscale materials, supraparticles exhibit unique features: first, they preserve nanoparticulate properties, such as nano-derived catalytic activity, while elevating particle sizes to the (lower) microscale.[10,11] Second, they often provide additional unexpected functionalities beyond the sum of properties of their constituent building blocks, such as an emergent internal porosity of the material[12–14] or a well-controllable 3-dimensional spatial distribution of catalytic spots within a supportive surrounding.[15–17] This ultimately permits the development of catalytic materials that exceed the limits of current ones in terms of activity, selectivity, and stability.[3,18] Therefore, their high potential for catalytic applications is beyond all doubt.[15,19–21]

Despite the great potential of supraparticles, their applicability for catalysis in fixed-bed reactors is still limited because of their still too-small microscale sizes. In these reactors, particle (or pellet) sizes of at least 0.5 to 2 mm are required to avoid massive pressure drops as well as particle losses.[22] While there have been a some attempts to create millimeter-sized supraparticles using nanoparticles as building blocks,[23–29] these suffer from several drawbacks such as poor upscalability, involvement of complex surfaces as synthesis platforms, or challenging template fabrication and removal steps, as well as limitations in the materials that can be used.

Therefore, we propose the concept of attaching supraparticles to beads using a binder material to create suprabeads that maintain the supraparticle features while providing high micron to millimeter sizes. The idea is being implemented in the development of supraparticle-based supported catalytically active liquid metal solutions (SCALMS).[30] This recently proposed new class of heterogeneous catalysts consists of small amounts of catalytically active species (such as Pd, Pt, Rh, or Ni) dissolved in an inactive low-melting-point metal (such as Ga) supported by a porous inert material (such as SiO_2, Al_2O_3 or SiC).[6,31–34] At elevated temperatures ($T > 250$ °C), these alloys become fully liquid and thus the catalytically active metal is embedded in the highly dynamic matrix metal. The catalytic reaction occurs only at the liquid metal–gas interface (unlike conventional supported liquid phase catalysis). The liquid metal provides no reactant solubility and the active metal appears at the liquid surface as an active single atom during catalysis.[34] This high surface mobility is probably one of the main reasons for the high selectivity and excellent coking resistance of SCALMS in high-temperature dehydrogenation reactions, as shown for butane, propane, and methylcyclohexane dehydrogenation.[30,33,35,36]

Recent publications have highlighted the high potential of SCALMS while the deposition of gallium on porous supports remains an open challenge (if chemical Ga deposition *via* impregnation and decomposition of air-sensitive and expensive $(Et_3N)GaH_3$ is to be avoided) due to the high surface tension of gallium droplets and thus their poor wetting behavior and scarce intrusion into the pores of commonly used substrates.[37] This limitation can be overcome by using the building block approach to create supraparticles. It allows us to pursue gallium particle encapsulation by a porous support matrix (Fig. 1(a) and (b)): single support nanoparticles act as a scaffold in which the gallium is trapped during supraparticle synthesis *via* spray-drying, which is a forced assembly of nanoparticles within a droplet (Fig. S1, ESI†). In the next step, the catalytically active platinum species is deposited by galvanic displacement into the gallium contained in the supraparticles. This results in catalytically active supraparticles consisting of GaPt and SiO_2. For the applicability of these supraparticle-based SCALMS in propane dehydrogenation reactions, the subsequent generation of suprabeads using these supraparticles is essential. The suprabead envisaged as a SCALMS material (Fig. 1(c) and (d)) consists of an inert millimeter-sized (aluminum oxide) bead covered with supraparticles. Their attachment to the bead is ensured by an (alumina-based) binder material. The beads and binder are mixed and the so-coated beads are rolled in a bed of supraparticles.

Following the detailed procedure described in the Experimental Section (ESI†), the concept of suprabead fabrication is successfully implemented (initially without Pt) using supraparticles consisting of commercial SiO_2 and Ga nanoparticles synthesized *via* an ultrasonication procedure[37–39] (dynamic light scattering measurements and transmission electron microscopy of the nanoparticles are provided in ESI† Fig. S2). As shown in a scanning electron microscopy (SEM) study (Fig. 2(a)) as well as by nano X-ray computed tomography (nano-CT) (Fig. S3 and ESI† Videos 1–3), gallium particle encapsulation by a porous support matrix was successfully achieved during spray-drying.

The supraparticles obtained (hereafter referred to as Ga-SPs) possess an almost spherical shape and sizes of around 4 to 10 μm (confirmed by laser diffraction measurements (LDM) ESI† Fig. S4). It should be noted that the observed morphology of Ga-SPs is common for spray-dried assemblies: During droplet evaporation, the contained nanoparticles initially form a dense shell at the air/liquid interface. Further shrinkage of the droplet leads to a collapse of the spherical template structure and to the formation of the observed doughnut-like or sphere-like morphology with one or more craters.[40,41] The gallium nanoparticles are statistically distributed within the supraparticle with a SiO_2 to Ga weight ratio of $\sim$3.5 (calculated based on the Ga weight content of the sample as determined by inductively coupled plasma atomic emission spectroscopy (ICP-AES) ESI† Table S1). This statistical mixing of binary nanoparticle dispersion within a spray-dried supraparticle has already been extensively studied using models supported by experimental results.[42] The obtained Ga-SP-loaded suprabeads (hereafter referred to as Ga-SBeads) possess a spherical shape (Fig. 2(b)). They consist of a 0.73 mm alumina core, which is covered by an approximately 12 μm thick layer of supraparticles

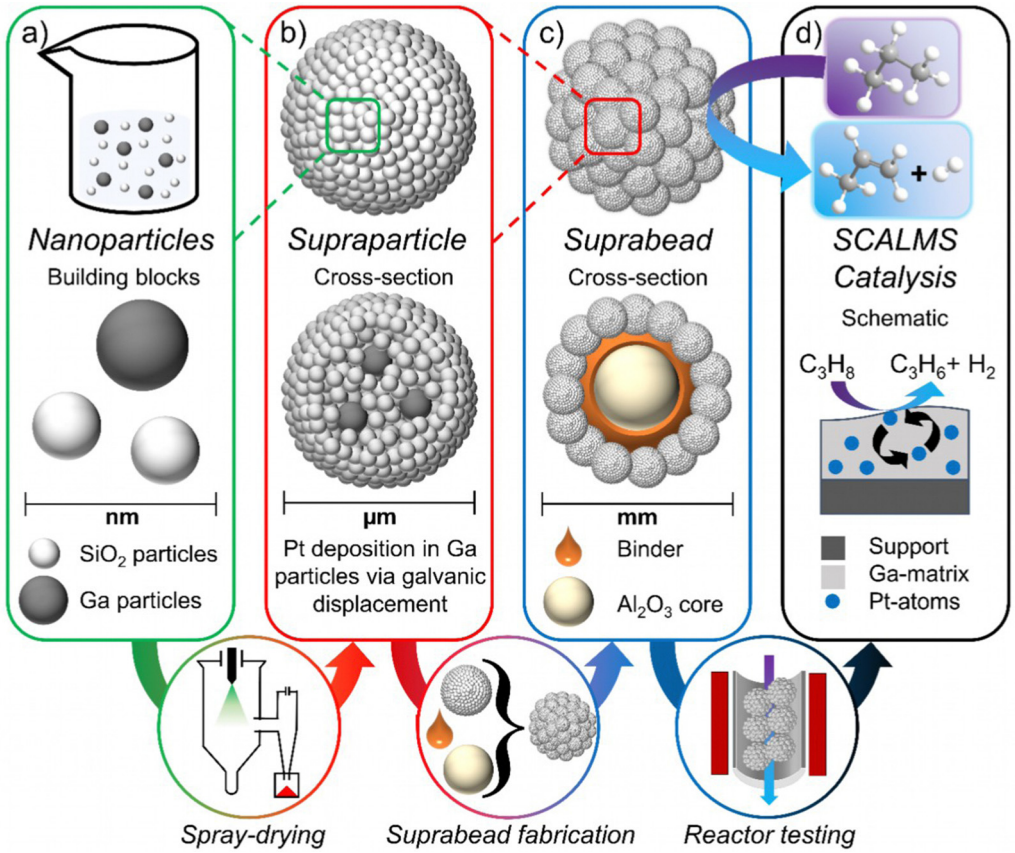

Fig. 1 Scheme showing the forced assembly of a mixed dispersion of gallium and silica nanoparticles (a) to supraparticles (b) *via* spray-drying. The supraparticles thus consist of gallium nanoparticles, which contain platinum (after its deposition *via* galvanic displacement) and are statistically distributed within a matrix consisting of silica nanoparticles. (Note that the perfect sphericity of the displayed schematic supraparticle shown does not exactly reflect its real morphology, but has been chosen for the sake of simplicity.) The supraparticles are subsequently attached to an aluminum oxide core using a binder, resulting in suprabeads (c). The suprabeads display a SCALMS material for catalytic propane dehydrogenation (d).

(without any specific ordered arrangement). The Ga-SBeads contain 11 weight-% Ga-SPs (see ESI† Table S2). The supraparticles are bonded to the core by an alumina binder, thus providing a uniform distribution of the supraparticle components (Ga and SiO_2) on its surface. Suprabeads providing complete coverage of the core with undamaged supraparticles and binder layer can only be obtained if the ratio of binder, core, and supraparticles is optimal, heat treatment during the fabrication is carefully conducted, and the supraparticles provide sufficient mechanical stability (examples for failed fabrication attempts are shown in ESI† Fig. S5).

The platinum deposition, essential for the SCALMS preparation, is realized on Ga-SPs by a galvanic displacement protocol,[43] and does not affect the structural properties of the supraparticles. In this context, it has to be mentioned that the synthesis of first Ga droplets and a later galvanic displacement reaction have been chosen to keep the SCALMS fabrication as close as possible to the established protocol.[37] The size, morphology, and pore characteristics of the obtained sample (hereafter referred to as Ga_{130}Pt-SP), remain comparable to those of Ga-SP (as shown by LDM ESI† Fig. S2, SEM ESI† Fig. S6, and nitrogen sorption measurements (NSM) ESI† Fig. S7). The same holds for the prepared Ga_{130}Pt-SP loaded suprabeads (Ga_{130}Pt-SBeads, SEM, and photograph ESI† Fig. S8). The envisaged approximate molar gallium-to-platinum ratio of 130 is achieved in Ga_{130}Pt-SBead (ESI† Table S1). This ensures that the Ga_{130}Pt alloy is liquid under the reaction conditions.[44] Comparing the pore characteristics of the supraparticles with the suprabeads (using NSM ESI† Fig. S9, and Table S3), the specific surface area S_{BET} and the total pore volume V_{pore} are both significantly reduced after suprabead fabrication due to the heavy macroporous/non-porous core material (a detailed explanation of the pore system characteristics of SPs and SBeads can be found in the ESI†). The mesopore network of the SPs in SBeads can be slightly infiltrated by binder material (resulting in slightly lowered mean pore diameters) while the general accessibility of these pores is still ensured.

Consequently, the material characterizations already indicate the presence and accessibility of GaPt within the millimeter-sized suprabeads. To demonstrate their usability as SCALMS catalysts, propane dehydrogenation reactions are carried out at 550 °C using a continuous gas-flow reactor. The detailed experimental procedure is described in the Experimental Section of the ESI† and a flow scheme of the reactor is shown in ESI† Fig. S10. For these catalytic experiments, three suprabead reproductions are delivered and two reference suprabead samples are used,

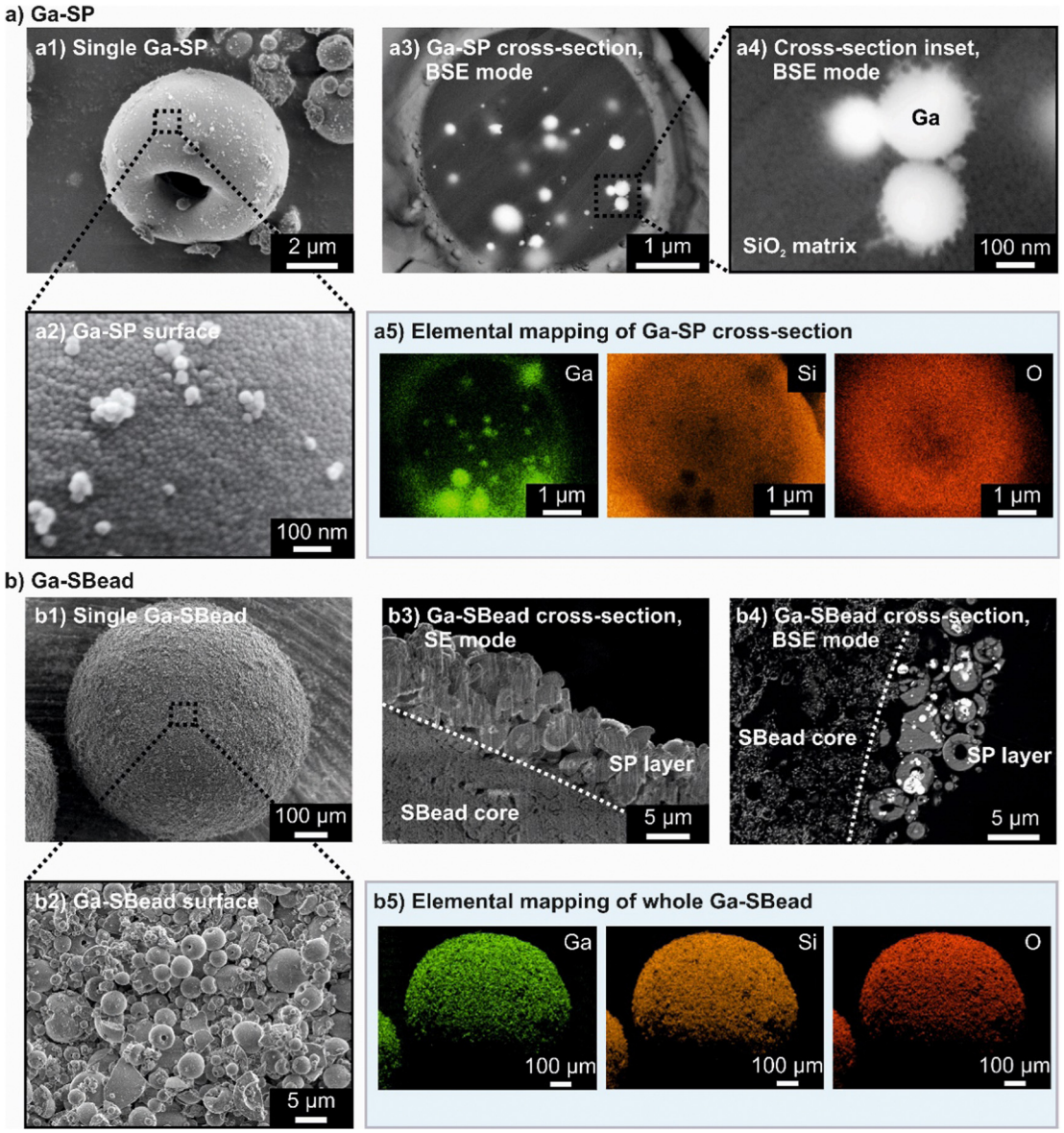

Fig. 2 SEM images of Ga-SP (a) and Ga-SBead (b), including micrographs showing their surface (a1, a2, b1, b2 – all secondary electron (SE) contrast), their cross-sections (a3 – backscattered electron (BSE) contrast, a4 - BSE, b3 – FIB cross-section SE, b4 – cross-section polish BSE) as well as elemental mappings of a Ga-SP cross-section (a5) and a whole Ga-SBead (b5).

namely Ga-SBeads and Pt-SBeads. The Pt-SBeads were prepared by wet impregnation of the SiO_2 supraparticles using a platinum precursor and subsequent reductive treatment to convert Pt(4+) into Pt(0) nanoparticles (which is an established route for the preparation of common heterogeneous Pt catalysts). This was followed by the fabrication of the suprabeads (referred to as Pt-SBeads). It should be noted that the gallium content of Ga-SBeads is comparable to that of Ga_{130}Pt-SBeads and the Pt content in the Pt-SBeads is even twice as much compared to the amount of Pt in the Ga_{130}Pt-SBeads (see ICP-AES, ESI† Table S1). The structural characterizations of the reference samples *via* NSM and SEM (shown in Fig. 2, as well as ESI† Fig. S7, Table S3, and Fig. S11) show similar morphologies and comparable pore characteristics.

The aim is to report for the first time the catalytic performance of GaPt SCALMS on suprabeads (Ga_{130}Pt-SBead-1, denoting the first of three reproductions of the Ga_{130}Pt-SBead synthesis) in comparison with the reference materials containing only one metal species (Ga-SBead and Pt-SBead). To confirm the absence of blind activity, the beads, and binder material without the metals were also tested under the same reaction conditions (ESI† Fig. S12). As shown in Fig. 3, Ga_{130}Pt-SBead-1 provides superior catalytic performance compared to the Pt-SBead and Ga-SBead materials. Ga-SBeads provide an initial conversion of 1.1% followed by a steady decline in activity over the remaining 15 h time-on-stream (TOS) to a final conversion value of 0.5%. Due to the oxophilic nature of gallium, the presence of a thin passivating Ga_2O_3 layer has been

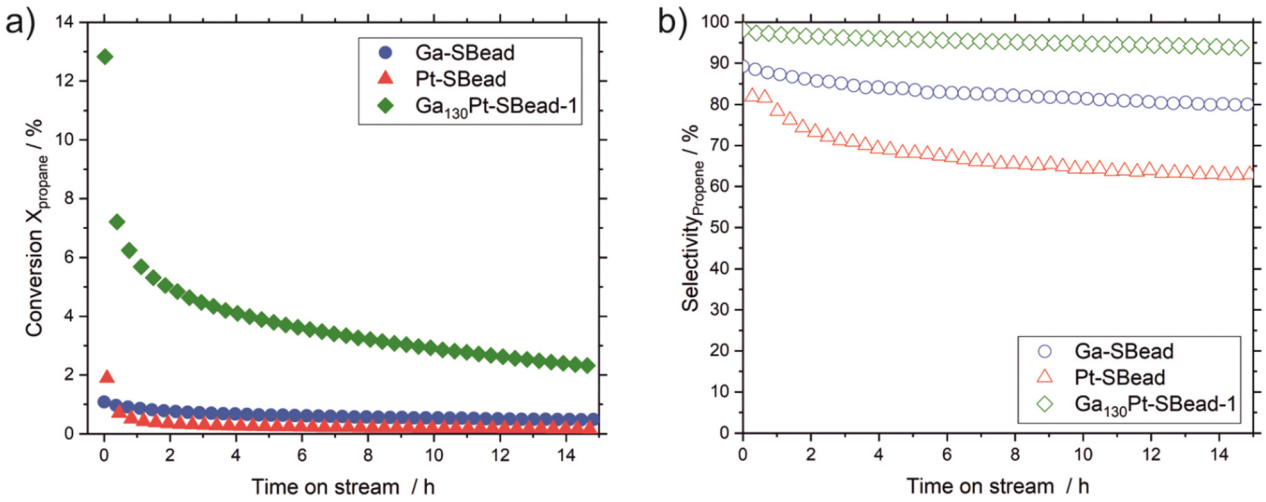

Fig. 3 Conversion (a; filled symbols) and selectivity (b; open symbols) for Ga-SBead (blue circles), Pt-SBead (red triangles), and Ga_{130}Pt-SBead-1 (green diamonds) in propane dehydrogenation. Catalyst mass in bed, 3 g. Pre-treatment conditions: 19.5 mL_N min^{-1} H_2, 80.5 mL_N min^{-1} Ar, 1.2 bar, 550 °C. PDH experiment: 8.9 mL_N min^{-1} C_3H_8, 89.9 mL_N min^{-1} Ar, 550 °C, 1.2 bar, 15 h TOS, GHSV: 1960 h^{-1}.

reported on gallium-based materials (regardless of the pre-activation step),[45] together with the presence of Lewis acidic Ga^{3+} sites.[46,47] Both species can activate hydrocarbon C-H bonds under these reaction conditions.[45,48,49]

The Pt-SBeads display an initial conversion of 1.89%, which deactivates rapidly to 0.4% and 0.1% after 1 h and 15 h of time-on-stream (TOS) respectively. The initial activity of the Pt-SBead is ascribed to the presence of Pt nanoparticles in the heterogeneous Pt based catalyst prepared by wet impregnation and subsequent reductive treatment. However, under reaction conditions, these Pt nanoparticles are prone to sintering due to weak metal–support interactions.[49] The process of sintering leads to the loss of active surface and the formation of vicinal sites. The later leads to cracking activity and coke formation which is responsible for the rapid deactivation observed with Pt-SBeads. Interestingly, the synergistic effects of combining Pt with Ga in the GaPt alloy lead to a significant jump in activity. Ga_{130}Pt-SBeads show an initial conversion of 12.8%. This represents a 6-fold and 12-fold increase in initial catalytic activity when compared to the Pt-SBeads and Ga-SBeads respectively, under the same reaction conditions. In addition, Ga_{130}Pt-SBeads display very high selectivity with an initial selectivity value of 98%. In contrast, Ga-SBeads show an initial selectivity value of 89%, representing a 9% decrease in selectivity compared to the alloy-based catalyst. The activity on Ga-SBeads induced by the presence of Ga_2O_3 is often accompanied by a tendency to crack,[48] which favors the enhanced formation of side products by Ga-SBeads and reduces their selectivity. The Pt-SBead sample shows a far lower selectivity of 82%, which decreases to 70% after 15 h TOS due to the presence of vicinal sites which promote side product formation and subsequent deactivation (note, blind activity shows a selectivity of 45%. ESI† Fig. S12). To further corroborate these results, two reproductions of Ga_{130}Pt-SBeads were made and tested for catalytic activity (and provided in ESI† Fig. S13).

The data obtained from structural characterization, metal loading, as determined by ICP-AES, and catalytic performance, as summarized in ESI† Table S4, strengthen our approach in the preparation of Ga_{130}Pt-SBeads and their excellent reproducibility. The nature of the active sites responsible for the activity in Ga_{130}Pt-SBeads is believed to be similar to that of already established GaPt SCALMS catalysts, since only its enclosure in the support was modified rather than the GaPt alloy. However, compared to established SCALMS, *e.g.*, Ga_{45}Pt SCALMS, the Ga_{130}Pt-SBeads presented here show superior activity (ESI† Fig. S14), which presumably results from the encasement of the GaPt droplets within the silica matrix of the supraparticles. This prevents migration and coalescence of GaPt droplets (both in the catalyst preparation process and the catalytic reaction) and thus, provides a higher catalytically active surface area. The still statistical distribution of Ga within the spent Ga_{130}Pt-SBeads (SEM ESI† Fig. S15) indicates the immobilization of the catalytically active phase. In GaPt SCALMS, the small amount of Pt present is alloyed with an excess of Ga. Under reaction conditions, the formed alloy becomes liquid.[50,51] In the presence of a hydrocarbon, the Pt metal is enriched at the liquid metal/gas interface.[30,34] The low solubility of the hydrocarbon ensures that subsequent substrate adsorption, reaction, and product desorption occur at the liquid metal/gas interface.[30,34] The absence of vicinal sites due to the isolated and atomically dispersed Pt within the Ga matrix prevents traditional deactivation by sintering. However, other deactivation phenomena may be responsible for the loss of activity seen in Ga_{130}Pt-SBeads. Obvious culprits could be changes in catalyst morphology. To investigate this further, analyses of the spent Ga_{130}Pt-Sbeads' structure provide no evidence of morphological or porosity changes (SEM ESI† Fig. S15 and NSM ESI† Fig. S16) - apart from minor supraparticle-losses. However, subatomic changes in the GaPt alloy under these conditions cannot be completely excluded. In addition, coke analysis was performed on the spent Ga-SBeads, Pt-SBeads, and Ga_{130}Pt-SBeads catalysts by temperature program oxidation (TPO). As shown in ESI† Fig. S17 Ga_{130}Pt-SBeads catalysts showed no detectable carbon

deposits, whereas Ga-SBeads and Pt-SBeads showed a mass loss of 0.04% and 0.1%, respectively. This suggests a different deactivation mechanism than coking. Raman *et al.* discussed other possible deactivation mechanisms at play, namely the phase separation of the alloy into Ga-rich and Pt-rich phases under reaction conditions.[37,52] Detailed studies of this phenomenon are currently underway as an extension of this work.

Conclusions

Taking advantage of the suprabead concept, we have succeeded in synthesizing a heterogeneous catalyst unit in which μm-scale catalytically active supraparticles are bound to mm-sized Al_2O_3 beads using an Al_2O_3-based binder. The supraparticles consist of GaPt nanoparticles enclosed by a matrix of SiO_2 nanoparticles, which was achieved by spray-drying a mixed dispersion of Ga and SiO_2 nanoparticles, followed by Pt deposition. The functionality and high performance of these novel SCALMS were demonstrated in the propane dehydrogenation reaction. The suprabead concept opens up a new world for the creation of supported catalytically active materials and for fully exploiting the high potential of supraparticles in catalysis.

Data availability

Data for this paper, including dynamic light scattering, ICP-AES, laser diffraction, nitrogen sorption, nano CT, propane dehydrogenation runs, photographs, SEM and EDX, TEM, and TPO measurements and analysis are available at Zenodo at **https://doi.org/10.5281/zenodo.8193496**.

Author contributions

This collaborative research was initiated by K. M., P. W., M. H., and S. W. General research goals were developed by S. W., M. H., T. Z., N. M., and P. G. The supervision of the whole project was done by S. W. and M. H. Performance of the syntheses and characterization were carried out as follows: Ga-nanoparticle dispersion was prepared by N. M., N. T. and N. D., spray-drying was carried out by P. G. and N. D. Suprabead development was conducted by T. Z., T. R. and N. D. Binder synthesis was done by T. Z. Propane dehydrogenation reactions were carried out by N. M. and N. D. Laser-diffraction was measured by T. Z. N_2 sorption measurements and analysis were performed by P. G. Cross-section preparation and analysis of SPs was conducted by P. G. SEM analysis of SPs and SBeads was performed by P. G. and T. R. Cross-section preparation and SEM imaging of SBeads and nano-CT experiments of SPs were performed by S. C. – the corresponding results were interpreted and discussed by S. C., B. A. Z. and E. S. Interpretation and conclusion of the results were done by S. W., M. H., T. Z., N. M., and P. G. Figures were created by T. Z., N. M., and P. G. The original manuscript draft was written by S. W. and N. M. with the contribution of T. Z., and P. G. Reviewing and editing were performed by T. R., K. M., P. W., and M. H. All authors proofread and commented on the manuscript.

Conflicts of interest

There are no conflicts to declare.

Acknowledgements

This work was financially supported by the Volkswagen Foundation (Experiment! grant 98498), and by Klaus Tschira Stiftung gGmbH (grant KT44), which are gratefully acknowledged. Financial support by the European Research Council (Project-ID 786475: Engineering of Supported Catalytically Active Liquid Metal Solutions) and by the Deutsche Forschungsgemeinschaft (DFG, German Research Foundation, SFB 1452, Project-ID 431791331) is also gratefully acknowledged. The authors thank BÜCHI Labortechnik GmbH for providing the spray-dryer equipment. Jakob Reichstein and Angelika Leistner (Chair of Physical Chemistry I, D. Guldi) are thankfully acknowledged for providing and conducting TEM analysis of Silica nanoparticles. The Institute of Particle Technology (LFG, W. Peukert) is thankfully acknowledged for granting access to dynamic light scattering measurement devices (Zetasizer Nano, Panalytical). The chair of Chemistry of Thin Films (CTFM, J. Bachmann) is thankfully acknowledged for granting access to the cross-section polisher IB-19530CP (JEOL). Quentin Vijverberg und Carmen Rubach (IMN & CENEM) are thankfully acknowledged for contributing to the SP nano-CT acquisition and the SBead cross-section preparation and analysis.

References

1 P. Sonström and M. Bäumer, Supported colloidal nanoparticles in heterogeneous gas phase catalysis: on the way to tailored catalysts, *Phys. Chem. Chem. Phys.*, 2011, **13**, 19270–19284.
2 C. Descorme, P. Gallezot, C. Geantet and C. George, Heterogeneous Catalysis: A Key Tool toward Sustainability, *ChemCatChem*, 2012, **4**, 1897–1906.
3 G. Prieto, J. Zečević, H. Friedrich, K. P. de Jong and P. E. de Jongh, Towards stable catalysts by controlling collective properties of supported metal nanoparticles, *Nat. Mater.*, 2013, **12**, 34–39.
4 G. Centi and J. Čejka, Needs and Gaps for Catalysis in Addressing Transitions in Chemistry and Energy from a Sustainability Perspective, *ChemSusChem*, 2019, **12**, 621–632.
5 C. H. Christensen, Catalysis for Sustainability, *Top. Catal.*, 2009, **52**, 205.
6 D. Astruc, Introduction: Nanoparticles in Catalysis, *Chem. Rev.*, 2020, **120**, 461–463.
7 M. J. Ndolomingo, N. Bingwa and R. Meijboom, Review of supported metal nanoparticles: synthesis methodologies, advantages and application as catalysts, *J. Mater. Sci.*, 2020, **55**, 6195–6241.

8 S. C. Glotzer and M. J. Solomon, Anisotropy of building blocks and their assembly into complex structures, *Nat. Mater.*, 2007, **6**, 557–562.
9 S. Wintzheimer, T. Granath, M. Oppmann, T. Kister, T. Thai, T. Kraus, N. Vogel and K. Mandel, Supraparticles: Functionality from Uniform Structural Motifs, *ACS Nano*, 2018, **12**, 5093–5120.
10 F. Iskandar, L. Gradon and K. Okuyama, Control of the morphology of nanostructured particles prepared by the spray drying of a nanoparticle sol, *J. Colloid Interface Sci.*, 2003, **265**, 296–303.
11 R. Vehring, W. R. Foss and D. Lechuga-Ballesteros, Particle formation in spray drying, *J. Aerosol Sci.*, 2007, **38**, 728–746.
12 J. Kim, O. Wilhelm and S. E. Pratsinis, Packaging of Sol-Gel-Made Porous Nanostructured Titania Particles by Spray Drying, *J. Am. Ceram. Soc.*, 2001, **84**, 2802–2808.
13 S. Wenderoth, G. Bleyer, J. Endres, J. Prieschl, N. Vogel, S. Wintzheimer and K. Mandel, Spray-Dried Photonic Balls with a Disordered/Ordered Hybrid Structure for Shear-Stress Indication, *Small*, 2022, **18**, e2203068.
14 S. Wintzheimer, M. Oppmann, M. Dold, C. Pannek, M.-L. Bauersfeld, M. Henfling, S. Trupp, B. Schug and K. Mandel, Indicator Supraparticles for Smart Gasochromic Sensor Surfaces Reacting Ultrafast and Highly Sensitive, *Part. Part. Syst. Charact.*, 2019, **36**, 1900254.
15 L. Gradon, R. Balgis, T. Hirano, A. M. Rahmatika, T. Ogi and K. Okuyama, Advanced aerosol technologies towards structure and morphologically controlled next-generation catalytic materials, *J. Aerosol Sci.*, 2020, **149**, 105608.
16 C. Chen, C. Nan, D. Wang, Q. Su, H. Duan, X. Liu, L. Zhang, D. Chu, W. Song, Q. Peng and Y. Li, Mesoporous Multicomponent Nanocomposite Colloidal Spheres: Ideal High-Temperature Stable Model Catalysts, *Angew. Chem.*, 2011, **123**, 3809–3813.
17 J. Reichstein, S. Schötz, M. Macht, S. Maisel, N. Stockinger, C. C. Collados, K. Schubert, D. Blaumeiser, S. Wintzheimer, A. Görling, M. Thommes, D. Zahn, J. Libuda, T. Bauer and K. Mandel, Supraparticles for Bare-Eye H 2 Indication and Monitoring: Design, Working Principle, and Molecular Mobility, *Adv. Funct. Mater.*, 2022, **32**, 2112379.
18 A. Fukuoka and P. L. Dhepe, Sustainable green catalysis by supported metal nanoparticles, *Chem. Rec.*, 2009, **9**, 224–235.
19 S. Wintzheimer, J. Reichstein, P. Groppe, A. Wolf, B. Fett, H. Zhou, R. Pujales-Paradela, F. Miller, S. Müssig, S. Wenderoth and K. Mandel, Supraparticles for Sustainability, *Adv. Funct. Mater.*, 2021, **31**, 2011089.
20 K. Hou, J. Han and Z. Tang, Formation of Supraparticles and Their Application in Catalysis, *ACS Mater. Lett.*, 2020, **2**, 95–106.
21 D. P. Debecker, S. Le Bras, C. Boissière, A. Chaumonnot and C. Sanchez, Aerosol processing: a wind of innovation in the field of advanced heterogeneous catalysts, *Chem. Soc. Rev.*, 2018, **47**, 4112–4155.
22 G. Eigenberger and W. Ruppel, *Ullmann's encyclopedia of industrial chemistry*, Wiley online library, Wiley-VCH, Weinheim, 7th edn, 2010.
23 N. Wu, H. Wei and L. Zhang, Efficient removal of heavy metal ions with biopolymer template synthesized mesoporous titania beads of hundreds of micrometers size, *Environ. Sci. Technol.*, 2012, **46**, 419–425.
24 D.-W. Lee, M.-H. Jin, C.-B. Lee, D. Oh, S.-K. Ryi, J.-S. Park, J.-S. Bae, Y.-J. Lee, S.-J. Park and Y.-C. Choi, Facile synthesis of mesoporous silica and titania supraparticles by a meniscus templating route on a superhydrophobic surface and their application to adsorbents, *Nanoscale*, 2014, **6**, 3483–3487.
25 J. Kim, W. Shim, S.-M. Jo and S. Wooh, Evaporation driven synthesis of supraparticles on liquid repellent surfaces, *J. Ind. Eng. Chem.*, 2021, **95**, 170–181.
26 V. N. Paunov, H. Al-Shehri and T. S. Horozov, Attachment of composite porous supra-particles to air-water and oil-water interfaces: theory and experiment, *Phys. Chem. Chem. Phys.*, 2016, **18**, 26495–26508.
27 V. Rastogi, S. Melle, O. G. Calderón, A. A. García, M. Marquez and O. D. Velev, Synthesis of Light-Diffracting Assemblies from Microspheres and Nanoparticles in Droplets on a Superhydrophobic Surface, *Adv. Mater.*, 2008, **20**, 4263–4268.
28 M. Sperling, H.-J. Kim, O. D. Velev and M. Gradzielski, Active Steerable Catalytic Supraparticles Shuttling on Preprogrammed Vertical Trajectories, *Adv. Mater. Interfaces*, 2016, **3**, 1600095.
29 X. Guo, N. Xue, M. Zhang, R. Ettelaie and H. Yang, A supraparticle-based biomimetic cascade catalyst for continuous flow reaction, *Nat. Commun.*, 2022, **13**, 5935.
30 N. Taccardi, M. Grabau, J. Debuschewitz, M. Distaso, M. Brandl, R. Hock, F. Maier, C. Papp, J. Erhard, C. Neiss, W. Peukert, A. Görling, H.-P. Steinrück and P. Wasserscheid, Gallium-rich Pd-Ga phases as supported liquid metal catalysts, *Nat. Chem.*, 2017, **9**, 862–867.
31 A. Søgaard, A. L. de Oliveira, N. Taccardi, M. Haumann and P. Wasserscheid, Ga-Ni supported catalytically active liquid metal solutions (SCALMS) for selective ethylene oligomerization, *Catal. Sci. Technol.*, 2021, **11**, 7535–7539.
32 M. Kettner, S. Maisel, C. Stumm, M. Schwarz, C. Schuschke, A. Görling and J. Libuda, Pd-Ga model SCALMS: Characterization and stability of Pd single atom sites, *J. Catal.*, 2019, **369**, 33–46.
33 M. Wolf, N. Raman, N. Taccardi, R. Horn, M. Haumann and P. Wasserscheid, Capturing spatially resolved kinetic data and coking of Ga-Pt supported catalytically active liquid metal solutions during propane dehydrogenation in situ, *Faraday Discuss.*, 2021, **229**, 359–377.
34 N. Raman, S. Maisel, M. Grabau, N. Taccardi, J. Debuschewitz, M. Wolf, H. Wittkämper, T. Bauer, M. Wu, M. Haumann, C. Papp, A. Görling, E. Spiecker, J. Libuda, H.-P. Steinrück and P. Wasserscheid, Highly Effective Propane Dehydrogenation Using Ga-Rh Supported Catalytically Active Liquid Metal Solutions, *ACS Catal.*, 2019, **9**, 9499–9507.
35 M. Wolf, N. Raman, N. Taccardi, M. Haumann and P. Wasserscheid, Coke Formation during Propane Dehydrogenation over Ga-Rh Supported Catalytically Active Liquid Metal Solutions, *ChemCatChem*, 2020, **12**, 1085–1094.

36 O. Sebastian, S. Nair, N. Taccardi, M. Wolf, A. Søgaard, M. Haumann and P. Wasserscheid, Stable and Selective Dehydrogenation of Methylcyclohexane using Supported Catalytically Active Liquid Metal Solutions – Ga 52 Pt/SiO 2 SCALMS, *ChemCatChem*, 2020, **12**, 4533–4537.

37 N. Raman, M. Wolf, M. Heller, N. Heene-Würl, N. Taccardi, M. Haumann, P. Felfer and P. Wasserscheid, GaPt Supported Catalytically Active Liquid Metal Solution Catalysis for Propane Dehydrogenation-Support Influence and Coking Studies, *ACS Catal.*, 2021, **11**, 13423–13433.

38 H. Song, T. Kim, S. Kang, H. Jin, K. Lee and H. J. Yoon, Ga-Based Liquid Metal Micro/Nanoparticles: Recent Advances and Applications, *Small*, 2020, **16**, e1903391.

39 A. Yamaguchi, Y. Mashima and T. Iyoda, Reversible Size Control of Liquid-Metal Nanoparticles under Ultrasonication, *Angew. Chem., Int. Ed.*, 2015, **54**, 12809–12813.

40 E. Lintingre, F. Lequeux, L. Talini and N. Tsapis, Control of particle morphology in the spray drying of colloidal suspensions, *Soft Matter.*, 2016, **12**, 7435–7444.

41 D. Sen, J. S. Melo, J. Bahadur, S. Mazumder, S. Bhattacharya, G. Ghosh, D. Dutta and S. F. D'Souza, Buckling-driven morphological transformation of droplets of a mixed colloidal suspension during evaporation-induced self-assembly by spray drying, *Eur. Phys. J. E: Soft Matter Biol. Phys.*, 2010, **31**, 393–402.

42 S. Zellmer, G. Garnweitner, T. Breinlinger, T. Kraft and C. Schilde, Hierarchical Structure Formation of Nanoparticulate Spray-Dried Composite Aggregates, *ACS Nano*, 2015, **9**, 10749–10757.

43 M. B. Ghasemian, M. Mayyas, S. A. Idrus-Saidi, M. A. Jamal, J. Yang, S. S. Mofarah, E. Adabifiroozjaei, J. Tang, N. Syed, A. P. O'Mullane, T. Daeneke and K. Kalantar-Zadeh, Self-Limiting Galvanic Growth of MnO 2 Monolayers on a Liquid Metal—Applied to Photocatalysis, *Adv. Funct. Mater.*, 2019, **29**, 1901649.

44 H. Okamoto, in *Numerical data and functional relationships in science and technology*, ed. B. Predel, H. Landolt, R. Börnstein, W. Martienssen and O. Madelung, Springer, Berlin, 1996, p. 494.

45 V. J. Cybulskis, S. U. Pradhan, J. J. Lovón-Quintana, A. S. Hock, B. Hu, G. Zhang, W. N. Delgass, F. H. Ribeiro and J. T. Miller, The Nature of the Isolated Gallium Active Center for Propane Dehydrogenation on Ga/SiO_2, *Catal. Lett.*, 2017, **147**, 1252–1262.

46 M. D. Dickey, Emerging applications of liquid metals featuring surface oxides, *ACS Appl. Mater. Interfaces*, 2014, **6**, 18369–18379.

47 J. Yan, Y. Lu, G. Chen, M. Yang and Z. Gu, Advances in liquid metals for biomedical applications, *Chem. Soc. Rev.*, 2018, **47**, 2518–2533.

48 I. Takahara, M. Saito, M. Inaba and K. Murata, Effects of Pre-Treatment of a Silica-Supported Gallium Oxide Catalyst with H 2 on Its Catalytic Performance for Dehydrogenation of Propane, *Catal. Lett.*, 2004, **96**, 29–32.

49 J. J. H. B. Sattler, J. Ruiz-Martinez, E. Santillan-Jimenez and B. M. Weckhuysen, Catalytic dehydrogenation of light alkanes on metals and metal oxides, *Chem. Rev.*, 2014, **114**, 10613–10653.

50 M. Grabau, S. Krick Calderón, F. Rietzler, I. Niedermaier, N. Taccardi, P. Wasserscheid, F. Maier, H.-P. Steinrück and C. Papp, Surface enrichment of Pt in Ga2O3 films grown on liquid Pt/Ga alloys, *Surf. Sci.*, 2016, **651**, 16–21.

51 T. Bauer, S. Maisel, D. Blaumeiser, J. Vecchietti, N. Taccardi, P. Wasserscheid, A. Bonivardi, A. Görling and J. Libuda, Operando DRIFTS and DFT Study of Propane Dehydrogenation over Solid- and Liquid-Supported Ga x Pt y Catalysts, *ACS Catal.*, 2019, **9**, 2842–2853.

52 C. Hohner, M. Kettner, C. Stumm, D. Blaumeiser, H. Wittkämper, M. Grabau, M. Schwarz, C. Schuschke, Y. Lykhach, C. Papp, H.-P. Steinrück and J. Libuda, Pt–Ga Model SCALMS on Modified HOPG: Thermal Behavior and Stability in UHV and under Near-Ambient Conditions, *J. Phys. Chem. C*, 2020, **124**, 2562–2573.